47. Bord S, Horner A, Beeton CA, Hembry RM, Compston JE. Tissue inhibitor of matrix metalloproteinase-1 (TIMP-1) distribution in normal and pathological human bone. *Bone* 1999;24: 229–235.

48. Breckon JJ, Papaioannou S, Meikle MC *et al.* Stromelysin (MMP-3) synthesis is up-regulated in estrogen-deficient mouse osteoblasts *in vivo* and *in vitro*. *J Bone Miner Res* 1999;14:1880–1890.

49. Panagakos FS, Kumar S. Modulation of proteases and their inhibitors in immortal human osteoblast-like cells by tumor necrosis factor-alpha *in vitro*. *Inflammation* 1994;18:243–265.

50. Lorenzo JA, Pilbeam CC, Kalinowski JF, Hibbs MS. Production of both 92- and 72-kDa gelatinases by bone cells. *Matrix* 1992;12:282–290.

51. Manara MC, Baldini N, Scotlandi K *et al.* Mar Reversal of malignant phenotype in human osteosarcoma cells transduced with the alkaline phosphatase gene. *Bone* 2000;26:215–220.

52. Veis A, Tompkins K, Healy KE *et al.* Specific amelogenin gene splice products have signaling effects on cells in culture and in implants *in vivo*. *J Biol Chem* 2000;275:41263–41272.

ORIGINAL PAPERS

Upregulation of Id2, an oncogenic helix-loop-helix protein, is mediated by the chimeric EWS/ets protein in Ewing sarcoma

Mariko Fukuma[1], Hajime Okita[1], Jun-ichi Hata[1] and Akihiro Umezawa[1,*]

Department of Pathology, Keio University School of Medicine, 35 Shinanomachi, Shinjuku-ku, Tokyo 160-8582, Japan

The chromosomal translocation specifically linked to the Ewing sarcoma family results in the generation of fusion proteins comprising the amino terminal portion of EWS and the DNA-binding domain of ets transcription factors. The EWS/ets chimeric proteins act as aberrant transcription factors leading to tumorigenic processes. We searched for genes specifically activated in Ewing sarcoma cells but not in other tumor cell lines using the gene array technique, and found significantly enhanced expression of the Id2 gene. High levels of Id2 transcripts were detected in Ewing sarcoma cell lines and tumor tissues. The EWS/ets chimeric proteins activated the Id2 gene via the 5'-upstream promoter sequence. Chromatin-immunoprecipitation revealed a direct interaction of EWS/Fli-1 with the promoter regions of the Id2, TGF-β type II receptor, cyclin D1, and c-myc genes. Since EWS/Fli-1 transactivates c-myc, a cooperative action of the chimeric protein and c-myc leads to overexpression of Id2. In the present study, we suggest that Id2 is a target of the chimeric proteins and that the c-myc/Id2 pathway plays a pivotal role in the tumorigenic processes provoked by EWS/ets proteins.
Oncogene (2003) **22**, 1–9. doi:10.1038/sj.onc.1206055

Keywords: Ewing sarcoma; Id2; EWS/ets; chimeric protein

Introduction

Ewing sarcoma and peripheral primitive neuroectodermal tumor (PNET) are referred to as the Ewing sarcoma family of tumors that encompasses a group of biologically identical small round cell tumors. Ewing sarcoma is the second most common solid tumor found in the bone and soft tissue of children and young adults. Despite advances in multimodal cancer therapy, the overall long-term survival rate is still less than 60% (Paulussen *et al.*, 2001). Owing to the lack of unequivocal lineage markers, the histogenesis of Ewing sarcoma remains controversial. A specific chromosomal translocation, t(11;22)(q24:q12), has been reported in more than 80% of Ewing sarcomas. This chromosomal translocation results in the fusion of the 5' segment of the EWS gene on chromosome 22 with the 3' segment of the Fli-1 gene on chromosome 11 (Delattre *et al.*, 1992). The EWS gene also fuses with other members of the ets family, for example, ERG (Sorensen *et al.*, 1994), ETV1 (Jeon *et al.*, 1995), FEV (Peter *et al.*, 1997), and E1AF, which we have reported previously (Urano *et al.*, 1996, 1998).

Ets oncoproteins contain an 85 amino acid long domain, called the ets-domain, which has been conserved among members of the ets family. With this domain they bind as monomers to core 5'-GGA(A/T)-3' sequences, and the flanking sequences of this core determine the affinity and specificity of ets proteins to these target sequences. The functional synergy between ets oncoproteins with other transcription factors such as AP-1, Sp-1, and c-myb has been reported (Wasylyk *et al.*, 1990; Gegonne *et al.*, 1993; Nelsen *et al.*, 1993; Pankov *et al.*, 1994). Ets family members are involved in the developmental processes of various lineages such as T cell, B cell, and neural cells. The EWS/ets chimeric proteins work as aberrant transcription factors that interfere with this legitimate development and lead to oncogenesis of Ewing sarcomas.

The target genes of EWS/ets oncoproteins have extensively been investigated to understand the tumorigenic mechanism in Ewing sarcoma. EWS/Fli-1 is a strong transactivator of the c-myc promoter (Bailly *et al.*, 1994). Several genes such as EAT-2 (Thompson *et al.*, 1996), stromelysin (Braun *et al.*, 1995), and fringe (May *et al.*, 1997) are reported to be upregulated, while TGF-β type II receptor (TGFβIIR) (Im *et al.*, 2000), p21 (Matsumoto *et al.*, 2001), and p57KIP2 (Dauphinot *et al.*, 2001) are downregulated. Furthermore, EWS/Fli-1 interacts with hsRPB7, a subunit of human RNA polymerase II (Petermann *et al.*, 1998), and the EWS/Fli-1 fusion protein alters the IGF-IR signaling pathway (Toretsky *et al.*, 1997).

Since the ets proteins augment expression of various types of transcription factors, we presumed that there would be other genes whose expression is modified by the occurrence of the chimeric proteins. We sought for genes specifically expressed in Ewing sarcoma and found enhanced expression of the Id2 gene. Id proteins are helix-loop-helix (HLH) proteins lacking the basic amino acid domain necessary to bind DNA. Id proteins

2

function in a dominant negative manner by sequestering ubiquitously expressed (eg, E12, E47, and E2-2) or cell-type restricted (eg, Tal-1 and MyoD) basic HLH transcription factors, thereby blocking the binding of dimerized basic HLH proteins to DNA. They regulate transcription factors that are involved in developmental processes such as myogenesis, neurogenesis, bone morphogenesis, lymphopoiesis hematopoiesis, and myeloid differentiation (Norton et al., 1998). In transgenic chicken embryos, the ectopic expression of Id2 converts ectodermal cells to a neural crest fate (Martinsen and Bronner-Fraser, 1998). Id2−/− mice lack lymph nodes and Peyer's patches, and show a reduced population of natural killer cells (Yokota et al., 1999). Id proteins are also involved in cellular proliferation processes. The growth-suppressive activity of retinoblastoma proteins (RB) is reversed by Id2 through physical interactions between those proteins (Iavarone et al., 1994). High levels of Id2 reverse the growth suppressive activity of cyclin-dependent kinase inhibitors, p16 and p21 (Lasorella et al., 1996). Furthermore, the oncoproteins of the myc family require Id2 to bypass the regulatory function of RB (Lasorella et al., 2000). Thus, Id2, a protein required to maintain the timing of differentiation in mammalian development, is also a potent effector in the tumorigenic process of human cancer. Here we demonstrate extremely high levels of Id2 expression in Ewing sarcomas, presumably caused by the direct interaction between EWS/ets chimeric proteins and the promoter region of the Id2 gene.

Results

Gene expression analysis with the human cDNA array

We employed a cDNA expression array system to search for candidate target genes of EWS/ets chimeric proteins. Gene expression profiles of NCR-EW2 with the EWS/Fli-1, W-ES with the EWS/ERG, and NCR-EW3 with the EWS/E1AF, and NCR-G3 embryonal carcinoma are shown in Figure 1. Significantly high levels of c-myc and cyclin D transcripts were detected in all the cells tested. However, the levels were somewhat lower in NCR-G3 than in Ewing sarcoma cells. The highest level of Id2 transcripts was detected in Ewing sarcoma cells (Figure 1a–c), while it was below detectable level in NCR-G3 (Figure 1d). As Id2 regulates cellular differentiation into various lineages, the extraordinarily high level of Id2 expression may play a crucial role in the tumorigenesis of Ewing sarcoma. Similar levels of high expression were also seen in 40S ribosomal protein S-19, heat-shock 27 kD protein 1, glutathione S-transferase P, DNA-binding protein TAX and TAXREB67, RNA polymerase elongation factor SIII, guanine nucleotide-binding protein G-S, Y-box binding protein-1, proliferation-associated protein PAG, and thymosin beta-10 in all four cell lines. Why these transcripts increased still remains unclear.
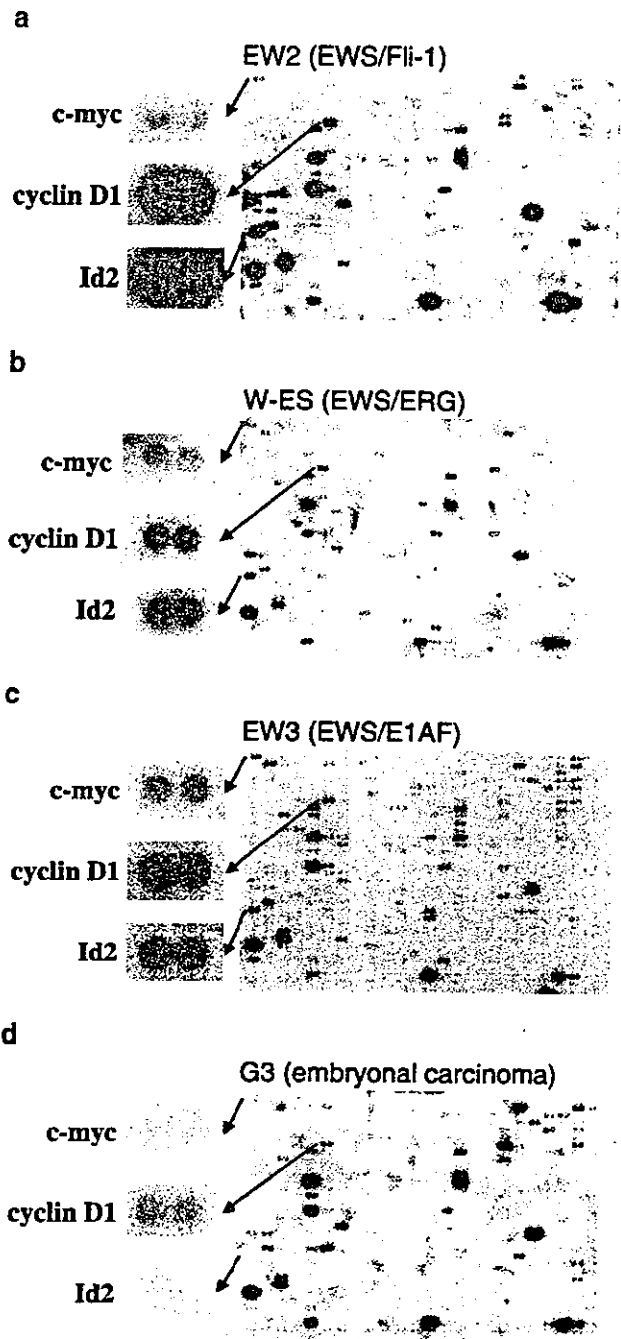

Figure 1 Gene expression profiles in Ewing sarcoma and embryonal carcinoma cells. ^{32}P-labeled cDNA probes were generated from each polyA$^+$ RNA sample isolated from the cells, NCR-EW2 with EWS-Fli-1 (a), W-ES with EWS/ERG (b), NCR-EW3 with EWS/E1AF (c), and NCR-G3 embryonal carcinoma (d). The spots of c-myc, cyclin D1 and Id2 are enlarged and shown on the left

Id2 expression in Ewing sarcoma

The enhanced expression of the Id2 gene was also detected by Northern blot analysis. Id2 was highly expressed in all the Ewing sarcoma cell lines, as well as in neuroblastoma cells, but was below a detectable level in NCR-G3 (Figure 2) and in HeLa cells (data not
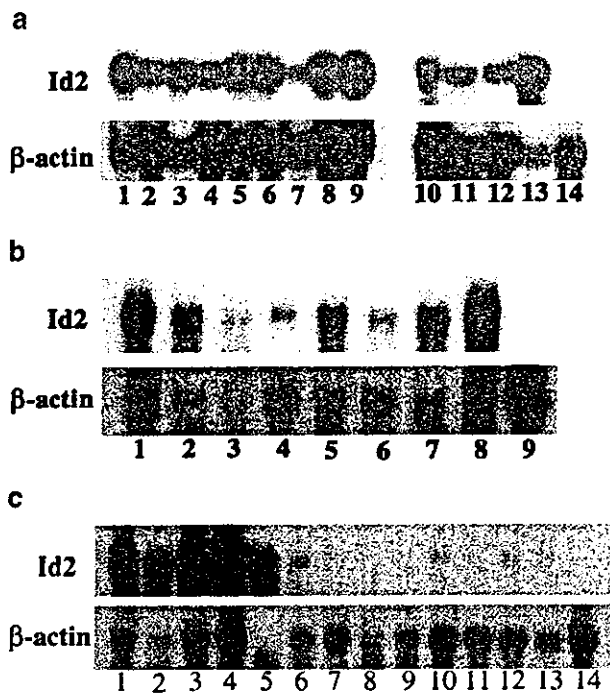
a

b

c

Figure 2 Northern blot analysis of Id2 expression. (a): Id2 transcripts in cell lines from Ewing sarcoma and other tumors. Lane 1: NCR-EW2 with EWS/Fli-1; Lane 2: NCR-EW3 with EWS/E1AF; Lanes 3 and 13: W-ES with EWS/ERG; Lane 4: SYM-1 with EWS/Fli-1; Lane 5: RD-ES with EWS/Fli-1; Lane 6: SCCH196 with EWS/Fli-1; Lane 7: EES-1 with EWS/Fli-1; Lane 8: EW93 with EWS/Fli-1; Lane 9: KU-9 with EWS/Fli-1; Lane 10: KNB-1 neuroblastoma; Lane 11: PN-1 (known chimera gene could not be detected); Lane 12: MURAOKA with EWS/Fli-1; Lane 14: NCR-G3 embryonal carcinoma. (b): Id2 transcripts in Ewing sarcoma tissue (Lanes 2–8: cases 1–7 in Table 2). Lane 1: NCR-EW2, Lane 9: NCR-G3. (c): Comparison of Id2 expression levels in tumor tissues. Lanes 2–5: cases 8,9,7 and 10 of Ewing sarcoma; Lanes 6–9: cases 11–14 of rhabdomyosarcoma; Lanes 10–14: cases 15–18 of neuroblastoma in Table 2. Lane 1: NCR-EW2 as a positive control

shown). Total RNA was also extracted from frozen blocks of tissues that had been diagnosed as Ewing sarcoma by immunohistochemistry and the detection of chimeric genes. Id2 was detected in all tissue samples from Ewing sarcoma. We further examined the expression of Id2 in comparison with other undifferentiated solid tumors in children, rhabdomyosarcoma, and neuroblastoma. Tumors are randomly selected from freeze-stock specimens. The chimeric genes in Ewing sarcoma specimens were found to be EWS/Fli-1. Significantly higher levels of Id2 transcripts were detected in Ewing sarcoma than in rhabdomyosarcoma and neuroblastoma. The high level of Id2 in Ewing sarcoma leads us to speculate that the EWS/ets gene products directly promote Id2 expression *in vivo*.

Activation of the Id2 promoter by the EWS/ets chimeric protein

We examined whether EWS/ets proteins activate the promoter of the Id2 gene. A DNA segment containing

the *cis*-regulatory element of Id2, nucleotide −221 to −46, was placed in either the forward (IdL-FWD) or reverse (IdL-REV) direction upstream of the luciferase gene. The reporter gene was co-transfected with an EWS/ets expression vector and phRL-TK reference vector. The luciferase activity was significantly enhanced with EWS/Fli-1, EWS/ERG, and EWS/E1AF (Figure 3a–c). The reversely ligated promoter produced almost the same results. This result is consistent with the fact that the upstream regulatory element usually works in either direction in the transcription process. Next, we introduced point mutations into the ets consensus sequence to analyze whether this sequence is required for the promoter activity (Figure 3d). The promoter region contains a canonical ets consensus sequence 50-bp downstream of the E-box where basic-HLH transcription factors interact. When the guanine (−156) was replaced with thymine the enhancing effect of EWS/Fli-1 decreased by about 25% (Figure 3e). Similar results were obtained when the adenine (−155) was replaced with cytosine. Thus, the ets consensus sequence is required to exert increased activation. When the adenine (−204) in the E-box was replaced with thymine, or thymine (−201) was replaced with cytosine, the promoter activity was significantly reduced by 80%. Similar results were obtained when EWS/E1AF was co-transfected as an effector (Figure 3f). Promoter activity was reduced by 30% after ets point mutation and by 70% after E-box mutation. A reporter construct IdS, lacking the E-box and juxtaposed sequences, was produced to allow analysis of the activation effect of chimeric proteins in the absence of E-box influence. Single nucleotide mutations in the ets site of the truncated promoter, at nucleotide positions −156 and −155, decreased the promoter activity by 46 and 45%, respectively (Figure 3g). These results imply that these two promoter elements, the E-box and the ets recognition sequence, contribute independently in the activation of the regulatory element of the Id2 gene.

The reporter genes were transfected into Ewing sarcoma cell lines to investigate whether they are functional in cells with native chimeric genes. In the NCR-EW2 cell line with EWS/Fli-1, both IdL and IdS were active (Figure 4a). The mutations at the ets site resulted in a decrease in activity by 30–40%. Similarly, in W-ES cells with EWS/ERG, the ets mutations diminished the promoter activity by 50–60% (Figure 4b). Owing to very low transfection efficiency no transcriptional activity was detected in NCR-EW3 cells with EWS/E1AF.

Binding of EWS/ets protein to the Id2 cis-regulatory element in vivo

We then used the chromatin immunoprecipitation (ChIP) technique to examine whether EWS/ets gene products interact with the Id2 promoter region. Chromatin was extracted from formaldehyde-treated cells, and anti-Fli-1 antibody or a corresponding amount of nonimmune IgG was added. Analysis by PCR detected
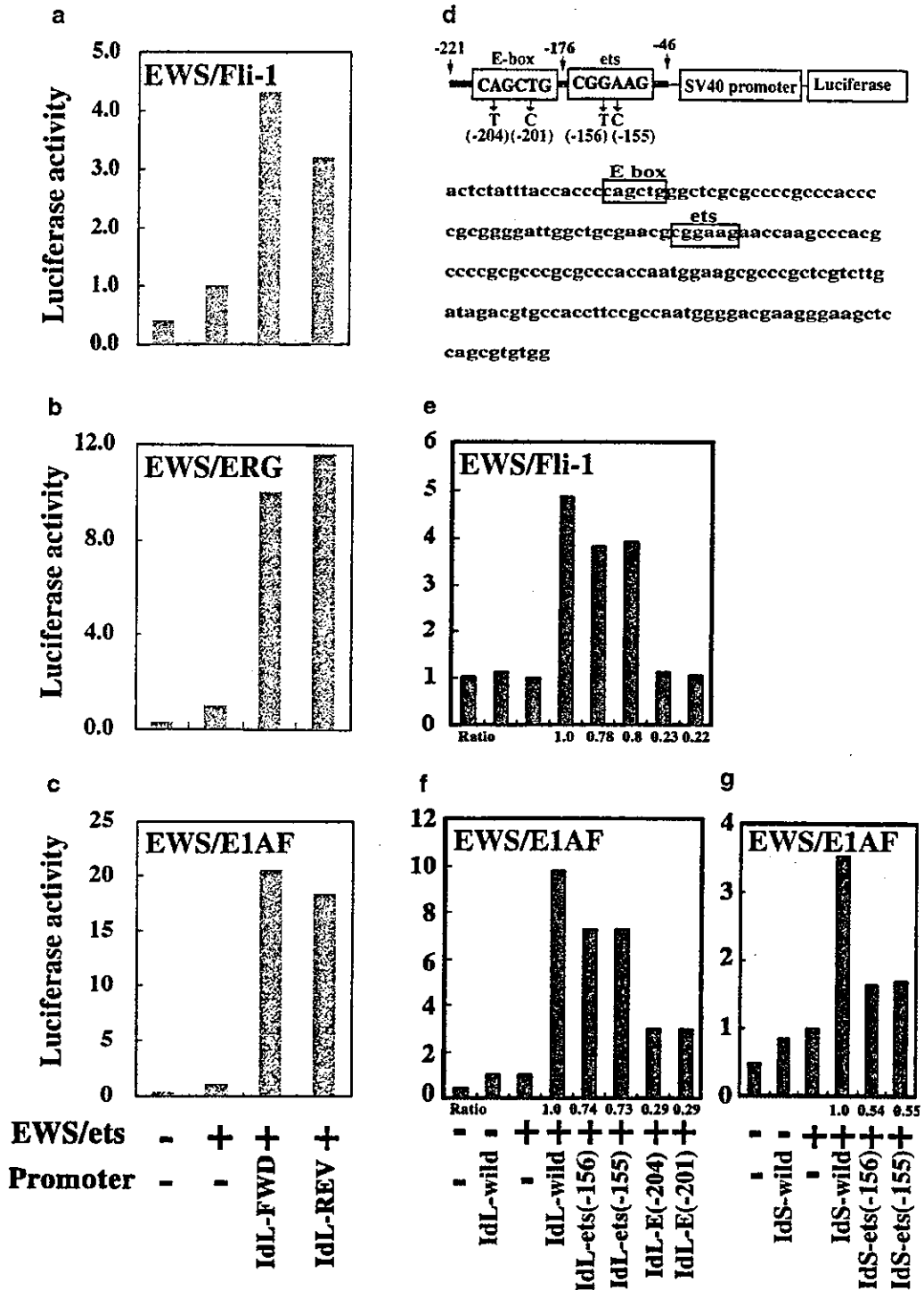
Figure 3 Transactivation of the Id2 promoter by the EWS/ets chimeric genes. HeLa cells were cotransfected with either Id2 promoter-luciferase reporter (IdL-FWD: forward, IdL-REV: reverse) or an empty reporter (pGL3-promoter vector), and an EWS/Fli-1 (a), EWS/ERG (b) or EWS/E1AF (c) expression vector. Furthermore, the phRL-TK vector was cotransfected to normalize the transfection efficiency. The luminescence intensity is expressed as a ratio of reporter vector to the phRL-TK reference vector. (d) The upstream regulatory region of the Id2 gene and the mutation map of the luciferase reporter gene. EWS/Fli-1 (e) or EWS/E1AF (f) was transfected as a transactivator of the mutant Id2 promoter. A comparison of the luciferase ratio of the mutated constructs and the wild-type promoter is shown at the foot of each column, and the wild type is regarded as 1.0 (e–g). (g) Reporter genes under the regulation of the truncated promoter sequence, −176 to −46, were cotransfected with EWS/E1AF into HeLa cells. Experiments were repeated at least three times and typical results are shown here

a

NCR-EW2 (EWS/Fli-1)

b
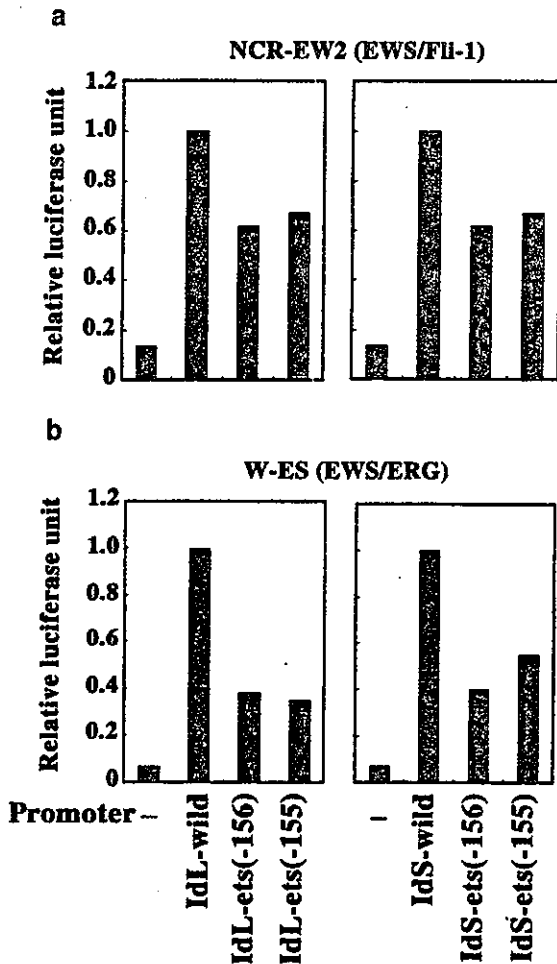
W-ES (EWS/ERG)

Promoter —

Figure 4 *cis*-transactivation of the Id2 promoter in Ewing sarcoma cells. Reporter genes were transfected into NCR-EW2 cells with EWS/Fli-1 (a) and into W-ES cells with EWS/ERG (b). The luminescence intensity is expressed as a ratio of reporter vector to the phRL-TK reference vector, and the wild type (IdL-wild or IdS-wild) is regarded as 1.0 Experiments were repeated twice and each experiment was performed on duplicate wells
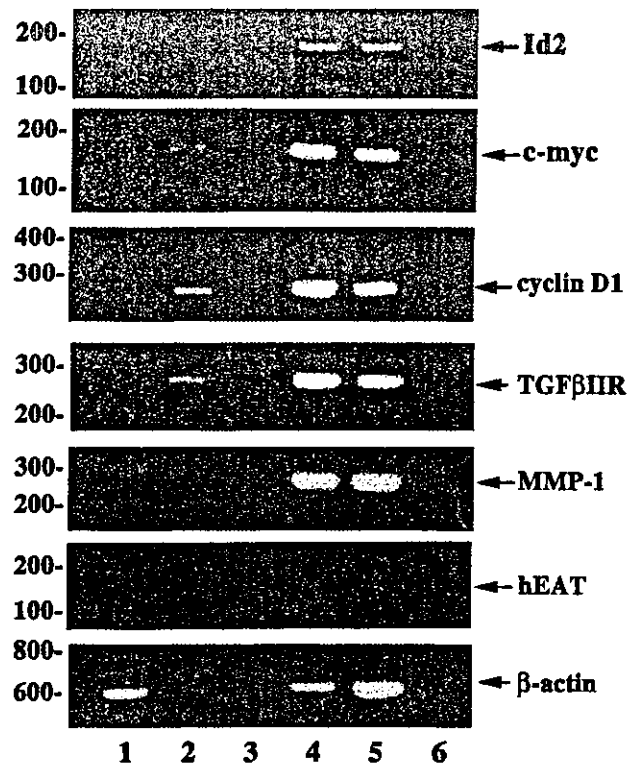

Figure 5 Binding of EWS/Fli-1 to the Id2 promoter *in vivo*. Crosslinked chromatin was prepared from NCR-EW2 cells. Chromatin was incubated with anti-Fli-1 antibody or normal rabbit IgG, and the regulatory fragments were amplified by PCR from the immunoprecipitates. The DNA templates are as follows: Lane 2, immunoprecipitates with anti-Fli-1; Lane 3, immunoprecipitates with normal rabbit IgG; Lane 4: chromatin DNA corresponding to 0.05% of total input DNA; Lane 5: chromatin DNA from human placenta; Lane 6: distilled H_2O as a negative control; Lane 1: molecular size markers. Molecular sizes are represented as base pair on the left of the panels

specific promoter regions of the Id2, *c*-myc, cyclin D1 and TGFβIIR genes in immunoprecipitates with anti-Fli-1 antibody but not with the nonimmune IgG (Figure 5). Neither the *cis*-element containing ets consensus sequences of EAT/MCL-1 nor of the matrix metalloproteinase-1 (MMP-1) was detected in either of the immunoprecipitates. Furthermore, the β-actin fragment was also undetected in either immunoprecipitate. These results indicate that the binding of the chimeric protein to the Id2 promoter region is specific. It is unlikely that the PCR products are from an intact Fli-1-chromatin complex, because Fli-1 transcripts are not detected in Ewing sarcoma cells (Bailly *et al.*, 1994), and a single band identical to the EWS/Fli-1 protein was detected in the immunoprecipitates from Ewing cells by the anti-Fli-1 antibody. We here demonstrate that the EWS/Fli-1 gene products interact directly with the regulatory elements of Id2, c-myc, cyclin D and TGFβIIR.

Discussion

In this study, we have demonstrated a direct transactivation of Id2 by EWS/ets chimeric proteins. Extremely high levels of Id2 gene expression were specifically observed in Ewing sarcoma cells and tumor tissues but not in embryonal carcinoma cells, rhabdomyosarcoma or neuroblastoma. We have also presented evidence suggesting that the EWS/ets proteins activate the Id2 gene through the direct interaction between the Id2 promoter and EWS/Fli-1 *in vivo*.

The substantial increase of Id2 by the EWS/ets chimeric proteins seemed to be functionally mediated through ets recognition sequences and E-box. Three E-box/ets clusters and several other ets-like sequences exist in the 2-kb enhancing region of the Id2 gene. The E-box located 50-bp upstream of the ets consensus sequence is important for the Id2 promoter activity. The decrease in Id2 promoter activity caused by point mutations in the E-box suggests that E-box-binding proteins, predominantly c-myc, and ets proteins, contribute to upregulating Id2 expression. The synergism of the ets proteins with other transcription factors such

as AP-1 (Wasylyk et al., 1990; Pankov et al., 1994), Sp-1 (Seth et al., 1993), and c-myb (Dudek et al., 1992) has been reported. In addition, DNA-binding motifs, that is, AP2, CEBP, GRE, E-box, CREB, AP-1, and SP-1, correlate with enhanced ets activity (Edelman et al., 2000). As the recognition sequence of SP-1 is located only 30-bp upstream of the ets site in the Id2 promoter, it is suggested that the EWS/ets chimeric proteins may cooperate with SP-1 to enhance the transcriptional activity of Id2. The cooperative effect of ets and E-box-binding proteins with other transcriptional factors is supposed to be crucial to Id2 transactivation, which subsequently contributes to tumor progression.

The high level of Id2 expression may explain certain characteristics of Ewing sarcoma such as primitive morphological features and expression of neural molecules. Several neural antigens are detectable by immunohistochemical analysis in Ewing sarcoma. However, few muscular antigens are detected (Sugimoto et al., 1997). Id proteins interact with ubiquitous bHLH class A proteins, such as E12 and E47, to block the formation of heterodimers of class A proteins and tissue-specific class B proteins, for example Tal-1 and MyoD (Benezra et al., 1990; Langlands et al., 1997). The Id2 expression induced by the specific chimeric proteins thus prevents expression of muscular phenotypes in the Ewing sarcoma. However, expression of Id2 in neurogenesis and during retinoic acid-induced differentiation of neuroblastoma suggests that Id2 is not a general inhibitor of differentiation in neural cell types (Neuman et al., 1993). The neurogenic potential of Ewing sarcoma may be explained by the gaining of tumorigenicity in the process of neurogenic lineage or by the overexpression of Id2 influencing precursor cells of other lineages toward neural crest and neurogenic fates. The primitive morphological appearance in the Ewing tumor family may be attributed to the high levels of Id2 that interfere with the activities of lineage-specific genes to commit cells to terminal differentiation as shown schematically in Figure 6.

The high levels of Id2 may also explain the high malignancy and poor prognosis of this tumor. Id2 expression reverses the inhibition of cellular proliferation and the block in cell cycle progression because of direct interaction of Id2 with RB via disruption of heterodimerization between Rb and E2F (Lasorella et al., 1996). The RB mutant phenotypes, that is ectopic cellular proliferation, loss of differentiation, and cell death, are reported to manifest through uncontrolled Id2 activity in mice (Lasorella et al., 2000). The oncogenic process of Ewing sarcoma may attribute to the Id2-mediated inhibition of RB that has a tumor suppressive activity in a series of cancers.

c-myc, which functions as an oncogenic molecule and was particularly abundant as shown by the arrays of this study, is directly induced by EWS/ets chimeric oncoproteins (Bailly et al., 1994; Noguera et al., 1992). Id2 expression is transactivated by N-myc and c-myc through direct binding to the Id2 promoter. Id2 is
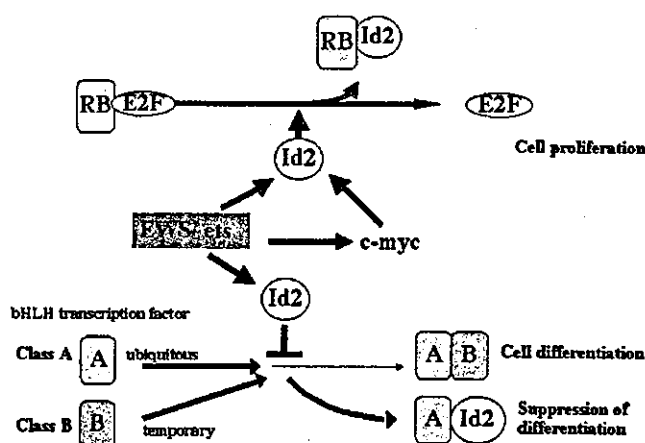

Figure 6 Possible function of EWS/ets chimeric proteins in tumorigenesis. EWS/ets fusion proteins activate the Id2 gene directly, and also indirectly as a result of activating c-myc gene. The higher levels of Id2 protein enhance cell cycle progression by inactivating RB protein family. Id2 protein, furthermore, interferes ubiquitous bHLH class A proteins to form heterodimers with tissue-specific class B proteins, and subsequently inhibits precursor cells to differentiate into a certain lineage

overexpressed in cells carrying extra copies of the N-myc gene in neuroblastoma and mediates signaling by myc proteins (Benezra et al., 1990). Thus, the induction of the Id2 gene seems to be augmented by myc oncoproteins that are upregulated by the EWS/ets chimeric proteins. Although further analyses are required, many essential molecules are involved in tumorigenic process executed by Id2 expression.

Based on the present experiments, we propose a possible role of EWS/ets chimeric proteins in oncogenesis of Ewing sarcoma (Figure 6). The chimeric proteins directly activate the Id2 gene. Moreover, they induce c-myc expression, with the subsequent high levels of c-myc further augmenting expression of Id2. Consequently, the high levels of Id2 interfere with the growth-suppressive activity of the RB protein family and the differentiation regulated by bHLH transcription factors.

Materials and methods

Cell lines and surgical samples

Surgical samples were obtained from patients with Ewing sarcoma. The cell lines used in this work and the specific fusion transcripts are shown in Table 1. Cells were cultured in RPMI medium supplemented with 10% fetal bovine serum. The surgically resected tumor was immediately frozen in OCT-compound (Miles Inc. Diagnostic Division, Elkhart, IN, USA) for immunohistochemical procedures and for RNA extraction. Diagnosis of Ewing sarcoma was immunohistochemically defined with an anti-p30/32^{MIC2} antibody, and detection of chimeric genes (EWS/Fli-1, EWS/ERG, or EWS/E1AF) was performed by a PCR technique using a specific set of primers described previously (Urano et al., 1998). Neuroblastoma and rhabdomyosarcoma were diagnosed by immunohistological examination. The tumor specimens used in this work, and the specific fusion transcripts of Ewing sarcoma are shown in

-285-

Table 1 Cell lines and fusion transcripts

Cell line	Diagnosis	Fusion transcripts
NCR-EW2	Ewing	EWS exon7/Fli-1 exon 5
NCR-EW3	Ewing	EWS exon7/E1AFexon9
W-ES	Ewing	EWS exon 7/ERG exon 9
SYM-1	Ewing	EWS exon7/Fli-1 exon 5
RD-ES	Ewing	EWS exon7/Fli-1 exon 5
SK- ES1	Ewing	EWS exon7/Fli-1 exon 5
SCCH196	Ewing	EWS exon 7/Fli-1 exon 6
EES-1	Ewing	EWS exon7/Fli-1 exon 6
EW93	Ewing	EWS exon7/Fli-1 exon 6
KU-9	PNET	EWS exon 7/Fli-1 exon 5
PN-1	PNET	not detected
MURAOKA	PNET	EWS exon 10/Fli-1 exon 8
KNB-1	Neuroblastoma	
NCR-G3	Embryonal carcinoma	

PNET: peripheral primitive neuroectodermal tumor.

Table 2 Clinical details of solid tumors

Case	Age/sex	Origin	Diagnosis	Fusion transcripts
1	16y/M	Abdomen	Ewing	EWS exon7/Fli-1 exon 7
2	16y/F	Fibula	Ewing	EWS exon 7/Fli-1 exon 5
3	—/M	—	Ewing	EWS exon 7/Fli-1 exon 6
4	26y/M	—	Ewing	EWS exon 7/Fli-1 exon 6
5	—/F	Retroperitoneum	PNET	EWS exon 7/Fli-1 exon 5
6	6y/F	kidney	Ewing	EWS exon 7/Fli-1 exon 5
7	—/M	—	Ewing	EWS exon 7/Fli-1 exon 6
8	17y/F	Adrenal	Ewing	EWS exon 10/Fli-1 exon 8
9	4y/M	Chest wall	Ewing	EWS exon 7/Fli-1 exon 6
7	—/M	—	Ewing	EWS exon 7/Fli-1 exon 6
10	30y/M	Thigh	Ewing	EWS exon 7/Fli-1 exon 5
11	11y/F	Upper limb	Rhabdomyosarcoma	
12	1y/F	Tibia	Rhabdomyosarcoma	
13	1y/F	Neck	Rhabdomyosarcoma	
14	5y/—	Retroperitoneum	Rhabdomyosarcoma	
15	7m/F	—	Neuroblastoma	
16	7m/M	Adrenal	Neuroblastoma	
17	10m/M	—	Neuroblastoma	
18	—/M	—	Neuroblastoma	

M: male, F: female, —: missing data.

Table 2. This work was sanctioned by the Ethics Committee in the Keio University School of Medicine (#13–12).

Gene expression

Isolation of total RNA from Ewing sarcoma cells and tissues was performed using ISOGEN (Nippon Gene Co., Ltd, Tokyo, Japan), and the polyA⁺ RNA was purified using OligotexTM-dT30 (JSR Corporation, Tokyo, Japan). For investigating differential gene expression, Atlas cDNA Expression Arrays (#7740-1, CLONTECH Laboratories, Inc., CA, USA) were employed. Atlas Arrays were reused three times at most to maintain a high reliability of quantitative analysis. ³²P-labeled cDNA probes were generated from each polyA⁺ RNA sample and hybridized to the Array according to the manufacturer's instructions. The membranes were exposed on an imaging plate and the accumulated radioactivity of each spot was counted with a Bio Imaging Analyzer (BAS-III, Fuji Photo Film Co., Ltd, Tokyo, Japan). The values were normalized by the housekeeping genes spotted on the same

membrane. The membrane was also exposed to a Kodak BioMax Ms X-ray film for 1–7 days to obtain a gene expression profile. For Northern blot analysis, 10 μg of each total RNA sample was analyzed as described by Thomas (1980).

Luciferase reporter assay

The activation of the Id2 promoter was examined with a Dual Luciferase Promoter Assay System (Promega, Co., WI, USA). The promoter region was amplified by PCR with the sense and antisense primers, 5'-CCGCACTTACTGTACTGTACTC-3' and 5'-TGCTGAGCTAGCTGCGCTT-3', respectively. The PCR product was enzymatically digested with *Rsa* I and *Hae* III, and the 176-bp band from the position −46 to −221 relative to the start site of transcription was ligated into the pGL3-promoter vector. Point mutations were introduced into the promoter sequences of Id2 ligated to the luciferase reporter gene using the Gene Editor *in vitro* Site-Directed Mutagenesis System (Promega). Adenosine at the position −204 relative to

the transcription start site was replaced with thymine (−204A:T), or thymine at −201 was replaced with cytosine (−201T:C) to disrupt the E-box. The guanine at −156 was replaced with thymine (−156G:T), or the adenine at −155 was replaced with cytosine (−155A:C) to disrupt the ets recognition sequence. The sequence of the promoter was confirmed by DNA sequence analysis (MegaBACE 1000, Amersham Pharmacia Biotech, CA, USA). An EWS/Fli-1 expression vector (Type II: EWS exon 7/Fli-1 exon 5) was constructed as follows. A 1771-bp cDNA product was amplified from the NCR-EW2 cell line using PCR primers, sense: 5′-GGAAGGAGA-GAAAATGGCGTCC-3′ and antisense: 5′-CTCACAA-GATGCTAGGAGACTGAG-3′, and ligated into the pGEM-T-Easy vector. The 1.8-kb fragment from the *Not* I digests of this first vector construct was ligated into the *Not* I site of the expression vector pcDNA3 (Promega). After confirmation of incorporation of the cDNA construct by DNA sequencing, expression was analyzed in HeLa cells by Western blotting. An expression vector of the fusion protein, EWS/Fli-1, EWS/ERG (Ohno *et al.*, 1994) or EWS/E1AF (Urano *et al.*, 1996, 1998) was cotransfected with the luciferase-reporter vector into HeLa cells using Lipofectin Reagent (Life Technologies, MD, USA). The cells were also transfected together with TK-RL reference vector for the standardization of transfection efficiency. The cells were treated according to the directions of the manufacturer. The intensity of the luminescence was measured by a luminometer, GENE LIGHT 55 (Microtec Co., Ltd., Chiba, Japan), and expressed in the ratio of the first luminescence from the reporter gene to the second luminescence from the RL-TK reference gene.

Chromatin immunoprecipitation

The chromatin DNA that interacts with EWS/Fli-1 was detected according to the procedure as described (Moreno *et al.*, 1999) with minor modifications. Briefly, cells fixed with 1% formaldehyde were dispersed in cell lysis buffer [10 mM HEPES pH 7.5, 10 mM EDTA, 0.5 mM EGTA, 0.5% IGEPAL CA-330 (Sigma, St Louis, MO, USA), and Protease Inhibitor Cocktail (Roche Diagnostics GmbH, Mannheim, Germany)]. Nuclei were pelleted, lysed in RIPA buffer (50 mM Tris-HCl pH 7.5, 150 mM NaCl, 1% IGEPAL, 0.1% sodium dodecylsulfate, 0.5% deoxycholate, and Protease Inhibitor Cocktail), sonicated and centrifuged. The supernatant was used as chromatin solution. Anti-Fli-1 antibody (Santa Cruz Biotechnology, Inc., Santa Cruz, CA, USA) or the equivalent amount of rabbit IgG was added and Dynabeads Protein G (Dynal ASA, Oslo, Norway) was employed to precipitate the antigen. The pairs of sense and antisense primers for PCR used to detect the promoter regions were as follows, c-myc: 5′-CATGCGGCTCTCTTACTCTG-3′ and 5′-CGGAGATTA-GCGAGAGAGGA-3′; cyclin D1: 5′-ACTTCGGTGGTCTT-GTCCC-3′ and 5′-TCCAGCAGCAGCCCAAGAT-3′; TGF-βIIR: 5′-ACGTCGAGGAGAGGGAGAA-3′ and 5′-AGAT-GTGCGGGCCAGATGT-3′ ; MMP-1: 5′-GTCTCCTTCG-CACAC-3′ and 5′-CTCAGTGCAAGGTAA-3′; EAT/Mcl-1: 5′-TTTGAAAACCTGGGATTGAG-3′ and 5′-GGTCAAAT-GGAAGGAACTCA-3′; β-actin: 5′-CACCACACTCT-AC-CTCTCAAG3′ and 5′-GCCATAAAAGGCAACTTTCGG-3′. The primers for Id2 are stated above.

References

Bailly RA, Bosselut R, Zucman J, Cormier F, Delattre O, Roussel M, Thomas G and Ghysdael J. (1994). *Mol. Cell Biol.*, **14**, 3230–3241.
Benezra R, Davis RL, Lockshon D, Turner DL and Weintraub H. (1990). *Cell*, **61**, 49–59.
Braun BS, Frieden R, Lessnick SL, May WA and Denny CT. (1995). *Mol. Cell Biol.*, **15**, 4623–4630.
Dauphinot L, De Oliveira C, Melot T, Sevenet N, Thomas V, Weissman BE and Delattre O. (2001). *Oncogene*, **20**, 3258–3265.
Delattre O, Zucman J, Plougastel B, Desmeze C, Melot T, Peter M, Kovar H, Joubert I, de Jong P, Rouleau G, Aurias A and Thomas G. (1992). *Nature*, **359**, 162–165.
Dudek H, Tantravahi RV, Rao VN, Reddy ES and Reddy EP. (1992). *Proc. Natl. Acad. Sci. USA*, **89**, 1291–1295.
Edelman GM, Meech R, Owens GC and Jones FS. (2000). *Proc. Natl. Acad. Sci. USA*, **97**, 3038–3043.
Gegonne A, Bosselut R, Bailly RA and Ghysdael J. (1993). *EMBO J.*, **12**, 1169–1178.
Iavarone A, Garg P, Lasorella A, Hsu J and Israel MA. (1994). *Genes Dev.*, **8**, 1270–1284.
Im YH, Kim HT, Lee C, Poulin D, Welford S, Sorensen PH, Denny CT and Kim SJ. (2000). *Cancer Res.*, **60**, 1536–1540.

Jeon IS, Davis JN, Braun BS, Sublett JE, Roussel MF, Denny CT and Shapiro DN. (1995). *Oncogene*, **10**, 1229–1234.
Langlands K, Yin X, Anand G and Prochownik EV. (1997). *J. Biol. Chem.*, **272**, 19785–19793.
Lasorella A, Iavarone A and Israel MA. (1996). *Mol. Cell. Biol.*, **16**, 2570–2578.
Lasorella A, Noseda M, Beyna M, Yokota Y and Iavarone A. (2000). *Nature*, **407**, 592–598.
Martinsen BJ and Bronner-Fraser M. (1998). *Science*, **281**, 988–991.
Matsumoto Y, Tanaka K, Nakatani F, Matsunobu T, Matsuda S and Iwamoto Y (2001). *Br. J. Cancer*, **84**, 768–775.
May WA, Arvand A, Thompson AD, Braun BS, Wright M and Denny CT. (1997). *Nat. Genet.*, **17**, 495–497.
Moreno CS, Beresford GW, Louis-Plence P, Morris AC and Boss JM. (1999). *Immunity*, **10**, 143–151.
Nelsen B, Tian G, Erman B, Gregoire J, Maki R, Graves B and Sen R. (1993). *Science*, **261**, 82–86.
Neuman T, Keen A, Zuber MX, Kristjansson GI, Gruss P and Nornes HO. (1993). *Dev Biol*, **160**, 186–195.
Noguera R, Triche TJ, Navarro S, Tsokos M and Llombart BA. (1992). *Lab. Invest.*, **66**, 143–151.

Norton JD, Deed RW, Craggs G and Sablitzky F. (1998). *Trends Cell Biol.*, **8**, 58–65.

Ohno T, Ouchida M, Lee L, Gatalica Z, Rao VN and Reddy ES. (1994). *Oncogene*, **9**, 3087–3097.

Pankov R, Neznanov N, Umezawa A and Oshima RG. (1994). *Mol. Cell Biol.*, **14**, 7744–7757.

Paulussen M, Ahrens S, Dunst J, Winkelmann W, Exner GU, Kotz R, Amann G, Dockhorn-Dworniczak B, Harms D, Muller-Weihrich S, Welte K, Kornhuber B, Janka-Schaub G, Gobel U, Treuner J, Voute PA, Zoubek A, Gadner H and Jurgens H. (2001). *J. Clin. Oncol.*, **19**, 1818–1829.

Peter M, Couturier J, Pacquement H, Michon J, Thomas G, Magdelenat H and Delattre O. (1997). *Oncogene*, **14**, 1159–1164.

Petermann R, Mossier BM, Aryee DN, Khazak V, Golemis EA and Kovar H. (1998). *Oncogene*, **17**, 603–610.

Seth A, Hodge DR, Thompson DM, Robinson L, Panayiotakis A, Watson OK and Papas TS. (1993). *AIDS Res. Hum. Retroviruses*, **9**, 1017–1023.

Sorensen PH, Lessnick SL, Lopez-Terrada D, Liu XF, Triche TJ and Denny CT. (1994). *Nat. Genet.*, **6**, 146–151.

Sugimoto T, Umezawa A and Hata J. (1997). *Virchows Arch*, **430**, 41–46.

Thomas PS. (1980). *Proc. Natl. Acad. Sci. USA*, **77**, 5201–5205.

Thompson AD, Braun BS, Arvand A, Stewart SD, May WA, Chen E, Korenberg J and Denny C. (1996). *Oncogene*, **13**, 2649–2658.

Toretsky JA, Kalebic T, Blakesley V, LeRoith D and Helman LJ. (1997). *J. Biol. Chem.*, **272**, 30 822–30 827.

Urano F, Umezawa A, Hong W, Kikuchi H and Hata J. (1996). *Biochem. Biophy. Res. Commun.*, **219**, 608–612.

Urano F, Umezawa A, Yabe H, Hong W, Yoshida K, Fujinaga K and Hata J. (1998). *Jpn. J. Cancer Res.*, **89**, 703–711.

Wasylyk B, Wasylyk C, Flores P, Begue A, Leprince D and Stehelin D. (1990). *Nature*, **346**, 191–193.

Yokota Y, Mansouri A, Mori S, Sugawara S, Adachi S, Nishikawa S and Gruss P. (1999). *Nature*, **397**, 702–706.

Use of Isolated Mature Osteoblasts in Abundance Acts as Desired-Shaped Bone Regeneration in Combination With a Modified Poly-DL-Lactic-Co-Glycolic Acid (PLGA)-Collagen Sponge

KENSUKE OCHI,[1,2] GOUPING CHEN,[3] TAKASHI USHIDA,[4] SATOSHI GOJO,[5] KAORU SEGAWA,[6] HITOSHI TAI,[7] KENJU UENO,[7] HIROYUKI OHKAWA,[8] TAISUKE MORI,[1] AKIRA YAMAGUCHI,[9] YOSHIAKI TOYAMA,[2] JUN-ICHI HATA,[1] AND AKIHIRO UMEZAWA[1]*

[1]Department of Pathology, Keio University School of Medicine, Tokyo, Japan
[2]Department of Orthopaedics, Keio University School of Medicine, Tokyo, Japan
[3]Tissue Engineering Research Center, AIST, Amagasaki, Japan
[4]Biomedical Engineering Laboratory, Graduate School of Engineering, University of Tokyo, Tokyo, Japan
[5]Department of Cardiac Surgery, Saitama Medical Center, Saitama, Japan
[6]Department of Microbiology, Keio University School of Medicine, Tokyo, Japan
[7]Fuji-Gotemba Research Laboratories, Chugai Pharmaceutical Co., Ltd., Shizuoka, Japan
[8]Product Research Lab., Chugai Pharmaceutical Co., Ltd., Tokyo, Japan
[9]Division of Oral Pathology and Bone Metabolism, Nagasaki University Graduate School of Biomedical Sciences, Nagasaki, Japan

Controlled regeneration of bone or cartilage has recently begun to facilitate a host of novel clinical treatments. An osteoblast line, which we isolated is able to form new bone matrix in vivo within 2 days and exhibits a mature osteoblast phenotype both in vitro and in vivo. Using these cells, we show that cuboidal bones can be generated into a predesigned shaped-bone with high-density bone trabeculae when used in combination with a modified poly-DL-lactic-co-glycolic acid (PLGA)-collagen sponge. PLGA coated with collagen gel serves as a good scaffold for osteoblasts. These results indicate that mature osteoblasts, in combination with a scaffold such as PLGA-collagen sponge, show promise for use in a custom-shaped bone regeneration tool for both basic research into osteogenesis and for development of therapeutic applications.   J. Cell. Physiol. 194: 45–53, 2002.
© 2002 Wiley-Liss, Inc.

The concept of regenerative medicine refers to the cell-mediated restoration of damaged or diseased tissue, and practically, regeneration of bone and cartilage may be one of the most accessible approaches. Candidate cell sources for regeneration of tissue include embryonic stem cells, fetal cells or adult cells such as marrow stromal cells (Bianco and Robey, 2000), each of which has both benefits and drawbacks.

Multipotent mesenchymal stem cells have recently been isolated from adult marrow and were shown to proliferate extensively, and to maintain the ability to differentiate into multiple cell types such as osteoblasts, chondrocytes, and myoblasts in vitro (Umezawa et al., 1992; Pittenger et al., 1999; Bianco and Robey, 2000). We have also shown that stromal cells are able to generate cardiomyocytes and endothelial cells (Makino et al., 1999), neuronal cells (Kohyama et al., 2001), and adipocytes (Umezawa et al., 1991). Clinical trials have already been performed using marrow stromal cells to treat patients with osteogenesis imperfecta (Horwitz et al., 1999) and osteoporosis (Canalis, 2000; Rodan and Martin, 2000). Thus, marrow stromal cells are expected to be a good source of cell therapy in addition to embryonic stem cells and fetal cells (Pittenger et al., 2000).

© 2002 WILEY-LISS, INC.

Humoral factors have also been used to induce bone formation (Yamaguchi et al., 2000). Bone morphogenetic proteins (BMPs) such as BMP-7 and BMP-2 induce osteogenesis in vivo when added them to matrix implants (Service, 2000). Treatment of simple collagen matrices with BMPs prompted rapid healing of bone defects in animal models. In human, implants of a

*Correspondence to: Akihiro Umezawa, Department of Pathology, Keio University, School of Medicine, 35 Shinanomachi, Shinjuku-ku, Tokyo, 160-8582, Japan.
E-mail: umezawa@1985.jukuin.keio.ac.jp

collagen matrix with BMP-2 and BMP-7 generate new bone as well as, or better than, autografts of healthy bone transplanted from another part of the patient's body. However, extremely high quantities of BMPs are needed to produce bone matrix, which is a major limitation to this approach (Service, 2000).

A third element required for in vivo bone formation, in addition to stem cells and cytokines, is a matrix or scaffold (Chen et al., 2000a,b). In an attempt to use the stromal system to direct clinical osteogenesis, marrow stromal cells implanted on gelatin sponges were shown to repair a craniofacial defect (Krebsbach et al., 1998; Tabata et al., 2000). Stromal cells implanted on hydorxyapatite/tricalcium phosphate ceramics also regenerated a critical size defect in the tibia, and resulted in consistent bone formation (Krebsbach et al., 1997). Various types of biomaterials as a scaffold is necessary for the successful tissue engineering (Ohgushi and Caplan, 1999).

In the present study, we show that clonal stromal cells can generate bone of custom-shapes and sizes in combination with an appropriate scaffold, in this case poly-DL-lactic-co-glycolic acid (PLGA)-collagen sponge.

MATERIALS AND METHODS
Cell culture

Primary culture of the marrow cells was performed according to Dexter's method (Dexter et al., 1977). Female C3H/He mice (n = 10) were anesthetized with ether, femurs were excised, and bone marrow cells were obtained for primary bone marrow cultures. Cells were cultured in Iscove's modified Dulbecco's medium (IMDM) supplemented with 20% fetal bovine serum (FBS) and penicillin (100 µg/ml)/streptomycin (250 ng/ml) at 37°C in humid air with 5% CO_2. Immortalized cells were obtained by frequent subculture for more than a year. Cell lines from different dishes were subcloned by limiting dilution. The screened line named KUSA/A1 was cultured in the maintenance medium consisting of IMDM supplemented with 10% FBS and penicillin (100 µg/ml)/streptomycin (250 ng/ml) at 37°C in humid air with 5% CO_2 as previously described (Umezawa et al., 1992). As for monolayer culture, KUSA/A1 cells was cultured with 50 µg/ml ascorbic acid and 10 mM sodium β-glycerophosphate in their culture media.

In vitro calcification assay and osteocalcin production

Cells were sonicated in the homogenization-buffer [20 mM Tris/HCl (pH 7.2), 0.1% Triton X-100] after washing twice with PBS. Calcium content in the culture was determined by CalciumC Test (Wako Chemical Co., Japan) according to the manufacturer's suggestion. The amount of osteocalcin into the culture media was determined by RIA using a mouse osteocalcin assay kit (Biomedical Technologies Inc., Stoughton, MA).

Measurement of alkaline phosphatase (ALP) and evaluation of parathyroid hormone (PTH) response

KUSA/A1 cells were analyzed by ALP assay as described (Leboy et al., 1991). PTH response was evaluated in KUSA/A1 cells as described (Sato et al., 1987).

Cytochemical and histochemical staining for ALP activity and β-galactosidase

Cells in 35 mm dishes were maintained in the standard media described above. Fixed cultures and sections were stained for 30 min at 37°C using naphthol AS-MX phosphate as a substrate and fast red violet LB salt as a coupler. Some cultures were maintained with standard media supplemented with 50 µg/ml ascorbic acid and 10 mM sodium β-glycerophosphate for up to 30 days in vitro. Sections were also stained with Xgal for 8 h at 37°C. Cells expressing β-galactosidase show a blue color after incubation with the Xgal substrate. In our hands, color formation was evident by 10–30 min incubation.

RNA extraction and Northern blotting

RNA was prepared by homogenizing the specimens in guanidinium isothiocyanate followed by centrifugation over a cesium chloride cushion as previously described (Umezawa et al., 1991). The RNA was then electrophoresed in a 1.0% agarose gel, transferred to a nylon filter (NEN Research Products, Boston MA), and hybridized with a murine collagen α2(I) (TIE5) cDNA probe (Amagai et al., 1989). The probe was labeled with [α-^{32}P]-CTP by the random-primer method (Feinberg and Vogelstein, 1983). Hybridization was carried out at 65°C for 14–16 h in a buffer containing five times SSPE (one time SSPE is 0.18 M NaCl, 10 mM NaH_2PO4/Na_2HPO_4 <pH 7.0>, pH 7.4, 1 mM EDTA), five times Denhardt's solution (one time Denhardt's solution is 0.02% Ficoll, 0.02% polyvinylpyrrolidone, 0.02% bovine serum albumin), 0.02% poly A, and 1% sodium dodecyl sulfate (SDS). The blots were washed with one time SSC containing 1% SDS at 65°C. The blots were exposed to X-ray film at −80°C using an intensifying screen.

Three dimensional collagen gel culture

KUSA/A1 cells were dispersely embedded in type I collagen gels. Eight volumes of cooled collagen solution (I-A Cellmatrix, Nitta gelatin, Osaka, Japan), one volumes of ten times concentrated IMDM medium, and one volume of buffer solution (0.05 N NaOH containing 2.2% $NaHCO_3$ and 200 mM HEPES) were added with gentle shaking on ice to ten volumes of IMDM medium suspension containing 10^7 cells/ml KUSA/A1 cells. Two hundred microliters of this medium-cell-collagen mixture was placed in each well of 96 well plastic microwell plate and allowed to gel by incubation at 37°C for 30 min. The gels were transferred to a 10 mm plastic dish and overlaid with 10 ml of IMDM containing 10% FBS. Cell cultures were incubated in 5% CO_2 at 37°C and the medium was changed every 3 days.

Introduction of the β-galactosidase gene

Recombinant adenovirus expressing bacterial β-galactosidase was prepared as described (Yamashita et al., 1999). Cells were infected by this virus at 10 plaque forming unit/cell. The expression of the β-galactosidase gene in KUSA/A1 was determined cytochemically in vitro. Nearly all the cells expressed β-galactosidase 3 days after transfection.

Inoculating of cells into syngeneic mice

Culture medium containing either KUSA/A1 cells (10^7 cells/ml) was injected to 8–12 weeks old female

collagen matrix with BMP-2 and BMP-7 generate new bone as well as, or better than, autografts of healthy bone transplanted from another part of the patient's body. However, extremely high quantities of BMPs are needed to produce bone matrix, which is a major limitation to this approach (Service, 2000).

A third element required for in vivo bone formation, in addition to stem cells and cytokines, is a matrix or scaffold (Chen et al., 2000a,b). In an attempt to use the stromal system to direct clinical osteogenesis, marrow stromal cells implanted on gelatin sponges were shown to repair a craniofacial defect (Krebsbach et al., 1998; Tabata et al., 2000). Stromal cells implanted on hydorxyapatite/tricalcium phosphate ceramics also regenerated a critical size defect in the tibia, and resulted in consistent bone formation (Krebsbach et al., 1997). Various types of biomaterials as a scaffold is necessary for the successful tissue engineering (Ohgushi and Caplan, 1999).

In the present study, we show that clonal stromal cells can generate bone of custom-shapes and sizes in combination with an appropriate scaffold, in this case poly-DL-lactic-co-glycolic acid (PLGA)-collagen sponge.

MATERIALS AND METHODS
Cell culture

Primary culture of the marrow cells was performed according to Dexter's method (Dexter et al., 1977). Female C3H/He mice (n = 10) were anesthetized with ether, femurs were excised, and bone marrow cells were obtained for primary bone marrow cultures. Cells were cultured in Iscove's modified Dulbecco's medium (IMDM) supplemented with 20% fetal bovine serum (FBS) and penicillin (100 μg/ml)/streptomycin (250 ng/ml) at 37°C in humid air with 5% CO_2. Immortalized cells were obtained by frequent subculture for more than a year. Cell lines from different dishes were subcloned by limiting dilution. The screened line named KUSA/A1 was cultured in the maintenance medium consisting of IMDM supplemented with 10% FBS and penicillin (100 μg/ml)/streptomycin (250 ng/ml) at 37°C in humid air with 5% CO_2 as previously described (Umezawa et al., 1992). As for monolayer culture, KUSA/A1 cells was cultured with 50 μg/ml ascorbic acid and 10 mM sodium β-glycerophosphate in their culture media.

In vitro calcification assay and osteocalcin production

Cells were sonicated in the homogenization-buffer [20 mM Tris/HCl (pH 7.2), 0.1% Triton X-100] after washing twice with PBS. Calcium content in the culture was determined by CalciumC Test (Wako Chemical Co., Japan) according to the manufacturer's suggestion. The amount of osteocalcin into the culture media was determined by RIA using a mouse osteocalcin assay kit (Biomedical Technologies Inc., Stoughton, MA).

Measurement of alkaline phosphatase (ALP) and evaluation of parathyroid hormone (PTH) response

KUSA/A1 cells were analyzed by ALP assay as described (Leboy et al., 1991). PTH response was evaluated in KUSA/A1 cells as described (Sato et al., 1987).

Cytochemical and histochemical staining for ALP activity and β-galactosidase

Cells in 35 mm dishes were maintained in the standard media described above. Fixed cultures and sections were stained for 30 min at 37°C using naphthol AS-MX phosphate as a substrate and fast red violet LB salt as a coupler. Some cultures were maintained with standard media supplemented with 50 μg/ml ascorbic acid and 10 mM sodium β-glycerophosphate for up to 30 days in vitro. Sections were also stained with Xgal for 8 h at 37°C. Cells expressing β-galactosidase show a blue color after incubation with the Xgal substrate. In our hands, color formation was evident by 10–30 min incubation.

RNA extraction and Northern blotting

RNA was prepared by homogenizing the specimens in guanidinium isothiocyanate followed by centrifugation over a cesium chloride cushion as previously described (Umezawa et al., 1991). The RNA was then electrophoresed in a 1.0% agarose gel, transferred to a nylon filter (NEN Research Products, Boston MA), and hybridized with a murine collagen $\alpha 2$(I) (TIE5) cDNA probe (Amagai et al., 1989). The probe was labeled with [α-^{32}P]-CTP by the random-primer method (Feinberg and Vogelstein, 1983). Hybridization was carried out at 65°C for 14–16 h in a buffer containing five times SSPE (one time SSPE is 0.18 M NaCl, 10 mM NaH_2PO4/Na_2HPO_4 <pH 7.0>, pH 7.4, 1 mM EDTA), five times Denhardt's solution (one time Denhardt's solution is 0.02% Ficoll, 0.02% polyvinylpyrrolidone, 0.02% bovine serum albumin), 0.02% poly A, and 1% sodium dodecyl sulfate (SDS). The blots were washed with one time SSC containing 1% SDS at 65°C. The blots were exposed to X-ray film at −80°C using an intensifying screen.

Three dimensional collagen gel culture

KUSA/A1 cells were dispersely embedded in type I collagen gels. Eight volumes of cooled collagen solution (I-A Cellmatrix, Nitta gelatin, Osaka, Japan), one volumes of ten times concentrated IMDM medium, and one volume of buffer solution (0.05 N NaOH containing 2.2% $NaHCO_3$ and 200 mM HEPES) were added with gentle shaking on ice to ten volumes of IMDM medium suspension containing 10^7 cells/ml KUSA/A1 cells. Two hundred microliters of this medium-cell-collagen mixture was placed in each well of 96 well plastic microwell plate and allowed to gel by incubation at 37°C for 30 min. The gels were transferred to a 10 mm plastic dish and overlaid with 10 ml of IMDM containing 10% FBS. Cell cultures were incubated in 5% CO_2 at 37°C and the medium was changed every 3 days.

Introduction of the β-galactosidase gene

Recombinant adenovirus expressing bacterial β-galactosidase was prepared as described (Yamashita et al., 1999). Cells were infected by this virus at 10 plaque forming unit/cell. The expression of the β-galactosidase gene in KUSA/A1 was determined cytochemically in vitro. Nearly all the cells expressed β-galactosidase 3 days after transfection.

Inoculating of cells into syngeneic mice

Culture medium containing either KUSA/A1 cells (10^7 cells/ml) was injected to 8–12 weeks old female

C3H/He mice subcutaneously. The tumors were harvested and fixed in 20% formalin 1 day to 8 weeks after the inoculation. Serial paraffin sections were prepared and stained with either hematoxylin and eosin (H&E), von Kossa or Toluidine Blue stain.

In vivo culture in diffusion chamber

Paired diffusion chambers were constructed using lucid rings and 0.45 µm membrane filters (Millipore Corporation, Bedford, MA) (Urist et al., 1982). The chambers shared a common filter. One chamber contained either KUSA/A1 cells in 200 µl aliquots from six dishes of confluent cultures. After receiving the contents, chambers were implanted subcutaneously in 8–12 weeks old female C3H/He mice. The animals were sacrificed after 2–8 weeks. The chambers were fixed in 20% formalin. Serial paraffin sections were prepared and stained with either hematoxylin and eosin, von Kossa or Toluidine Blue stain.

Preparation of cells, staining procedures, and fluorescence activated cell analysis

All samples (KUSA/A1) were treated by water lysis. Cells, at a final concentration of 1×10^7/ml, were incubated with 1 µg/µl monoclonal antibodies in Hank's balanced salt solution (containing 0.1% albumin and 0.1% sodium azide). In case that the first antibody is conjugated with biotin, cells were washed twice and incubated with streptoavidin-phycoerythrin (Gibco-BRL, Rockville, MD) for 30 min on ice. Purified antibodies in the first step were stained with FITC conjugated goat anti-mouse antibody. Antibodies (anti-mouse Flk-1, CD31, CD34, c-kit, Sca-1, CD140a, CD144, CD14, CD29, CD41, CD44, CD49b, CD49d, CD54, CD90, CD102, CD106, Ly-6C and Ly-6G, and isotype control antibodies) were purchased from Pharmingen Pharmaceutical, Inc. (San Diego, CA). After two washes with Hank's balanced salt solution, propidium iodide (PI) was added to each test tube at a concentration of 1 mg/ml just before acquisition by FACScan flow cytometry (Beckton Dickinson, Franklin Lakes, NJ) with the Argon laser at 488 nm. List mode data for 30,000–50,000 cells were collected in PI gate.

PLGA-collagen hybrid sponge preparation

Biodegradable hybrid sponge of PLGA (a 75:25 copolymer of lactic acid and glycolic acid with molecular weight of 90–126 kDa) and collagen was used as the three-dimensional porous scaffold for implantation (Chen et al., 2000a,b). The hybrid sponge was prepared by forming microsponges of collagen in the pores of PLGA sponge. At first, a PLGA sponge was prepared by a particulate-leaching technique using sieved sodium chloride particulates. PLGA polymer was dissolved in chloroform to prepare a PLGA solution in chloroform at a concentration of 20% (w/v). Sieved NaCl particulates (9.0 g), ranging in diameter from 355 to 425 µm, were added to the PLGA solution (5 ml), vortexed, and poured into an aluminum pan. The chloroform was allowed to evaporate by air-drying in a draft for 24 h and followed by 24 h of vacuum drying. The PLGA sponge with porosity of 90% and pore size of 355–425 µm was formed after NaCl particulates were leached out by washing with deionized water. Subsequently, the PLGA sponge

was immersed in a bovine collagen acidic solution (type I, pH 3.2, 5 µg/µl) under a vacuum so that the sponge pores filled with collagen solution. The collagen solution containing PLGA sponge was then frozen at −80°C for 12 h and lyophilized under a vacuum of 0.2 Torr for an additional 24 h to allow the formation of collagen microsponges in the sponge pores. Finally, the collagen microsponges were cross-linked by treatment with glutaraldehyde vapor saturated with 25% glutaraldehyde aqueous solution at 37°C for 4 h; and non-reacting aldehyde groups were blocked by treating with 0.1 M glycine aqueous solution. After washing with deionized water and lyophilizing, the PLGA-collagen hybrid sponge was prepared. The formation of collagen microsponge in the pores of PLGA sponge was confirmed by SEM observation. The hybrid sponge was sterilized using ethylene oxide.

Transplantation of cells in the PLGA sponge

KUSA/A1 suspension (10^7/ml) was injected gently into PLGA sponges. After injection, the sponges were incubated at 37°C for more than 30 min. Then the sponges were transplanted into subcutaneous tissue or abdominal cavity of mice. These operation plans are accepted by the Laboratory animal care and use committee of Keio University School of Medicine (#000024). All the experiments were followed by the guideline for the care and use of laboratory animals of Keio University School of Medicine.

RESULTS
Characterization of isolated differentiated osteoblasts

KUSA/A1 cells were originally isolated as cells which induce hematopoiesis in vivo (Umezawa et al., 1992). When cultured in monolayer, the cells were spindle-shaped in the growth phase and after confluence (Fig. 1A,B). Extracellular matrix positive for von Kossa stain appeared in cell culture and increased after confluence (Fig. 1C,D). Ultrastructurally, the matrix was electron dense and was clearly produced by the cells (Fig. 1E). RNA blot hybridization showed that the collagen α2(I) gene was expressed at a high level in KUSA/A1 cells, the same as in other stromal cell lines (Fig. 1F) (Umezawa et al., 1992).

We analyzed growth curve, ALP activity, in vitro calcification, osteocalcin (bone gla protein) release, and response to PTH in comparison with MC3T3-E1 cells. KUSA/A1 proliferation, which was measured by DNA content, was equivalent to that of MC3T3-E1 cells. ALP activity of KUSA/A1 cells in growth phase was approximately tenfold higher than in MC3T3-E1 cells (Fig. 1G). In vitro calcification, which steadily increased both before and after confluence, was approximately 100-fold higher after the confluent stage in KUSA/A1 cells than in MC3T3-E1 cells (Fig. 1H). Osteocalcin release into culture media peaked on day 5 in KUSA/A1 cells and was two- to threefold higher than in MC3T3-E1 cells (Fig. 1I). PTH response, measured as cAMP production, gradually decreased during the culture period in KUSA/A1 cells but increased in MC3T3-E1 cells (Fig. 1J). This response to PTH did not require any induction and was independent of culture conditions.
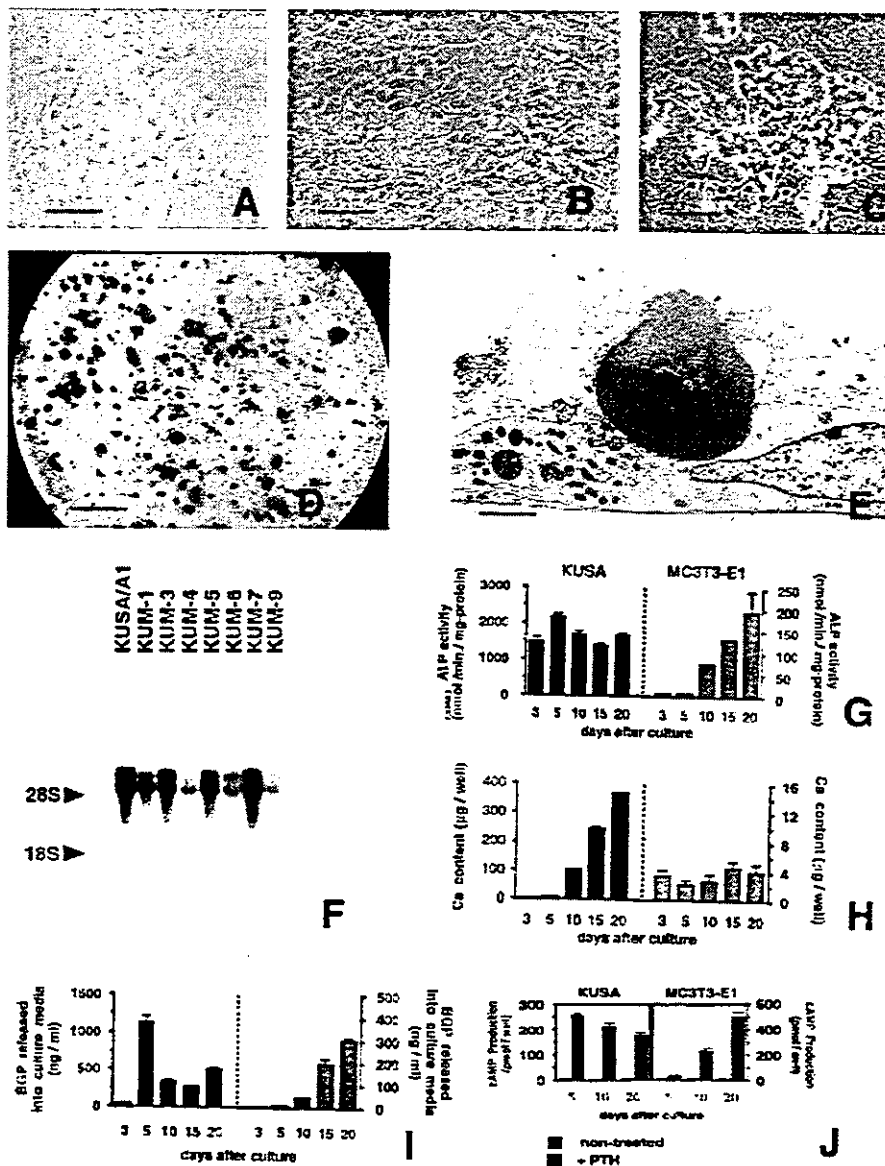
Fig. 1. In vitro characteristics of KUSA/A1 cells as a mature osteoblast model. A: Phase contrast micrograph of KUSA/A1 cells at the semiconfluent stage. B: KUSA/A1 cells 7 days postconfluence. C: Extracellular matrix produced from KUSA/A1 cells. D: Calcium deposition in KUSA/A1 culture. KUSA/A1 cells cultured in supplemented medium containing β-glycerophosphate were fixed and stained in situ by the von Kossa technique. E: Transmission electron micrograph of the extracellular matrix produced by KUSA/A1.

F: Expression of the collagen α2(I) gene in marrow stromal cell lines (Umezawa et al., 1992). G: ALP activity in KUSA/A1 cells and MC3T3-E1 cells. H: Quantitative analysis of calcium deposition in KUSA/A1 cells and MC3T3-E1 cells. I: Bone Gla protein (osteocalcin) secretion in KUSA/A1 cells and MC3T3-E1 cells. J: cAMP production after PTH treatment. PTH response of KUSA/A1 cells was compared with that of MC3T3-E1 cells, as measured by cAMP production. Scale bars: 120 μm (A,B,C), 5 mm (D), 2 μm (E).

Three-dimensional culture of KUSA/A1 cells in collagen gels

To generate a three-dimensional cell culture system, KUSA/A1 cells were suspended and cultured in collagen gels (Fig. 2). Gels containing KUSA/A1 were transparent in vitro under a phase contrast microscopy on day 3 and remained semi-transparent until 2 weeks. Histologically, KUSA/A1 cells formed a reticular network, which had evidence of calcification by von Kossa

staining at 2 weeks. These cells exhibited high ALP activity. At 4 weeks, heavy calcium deposition had rendered the gels opaque, even though the cultures were not supplemented with β-glycerophosphate.

In vivo osteogenic activity in KUSA/A1 cells

To determine the potential osteogenic activity of KUSA/A1 in vivo, the cells were injected subcutaneously into syngeneic mice (Fig. 3A–E). Before inoculation,
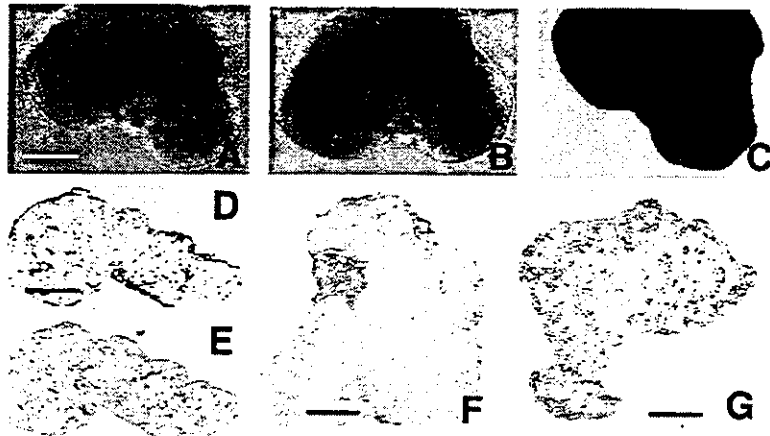
Fig. 2. Three-dimensional culture of KUSA/A1 cells in collagen gel. Phase contrast micrograph of three-dimensional culture of KUSA/A1 cells in collagen gel for 3 days (A), 2 (B), and 4 weeks (C). At 4 weeks, gels have become opaque. D: Microscopic examination of KUSA/A1 in collagen gels at 2 weeks. H&E stain. KUSA/A1 cells connected with each other and formed a reticular network. E: KUSA/A1 culture in collagen gels with von Kossa staining. The cells were cultured without β-glycerophosphate. F: ALP cytochemical staining of KUSA/A1 cells at 2 weeks. G: von Kossa staining of KUSA/A1 culture at 4 weeks. Scale bars: 170 μm (A,D,F,G).
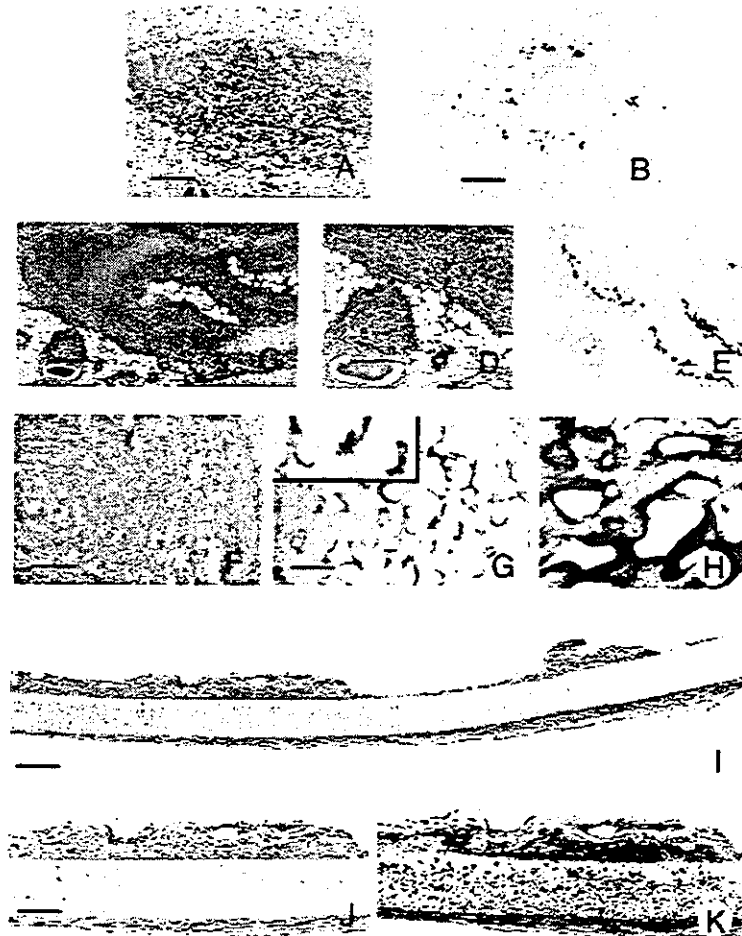

Fig. 3. Membranous ossification by KUSA/A1 in vivo. A and B: Microscopic examination of KUSA/A1 tumor in the subcutaneous tissue 2 days after injection. H&E stain (A) and von Kossa stain (B). Bone matrix was detected on day 2. C: KUSA/A1 tumor on day 3. H&E stain. D: Higher magnification of C. E: KUSA/A1 tumor on day 3 stained with von Kossa stain. Bone matrix had increased on day 3, as compared with day 2. F: Complete bone formation with a marrow cavity at 8 weeks. G: Enzyme histochemistry for β-galactosidase of KUSA/A1 tumor, 2 weeks after inoculation. Bone was generated by KUSA/A1 cells, which were transfected with β-galactosidase. H: Enzyme histochemistry for ALP of KUSA/A1 tumor, 2 weeks after injection. KUSA/A1 cells, which induce bone, were strongly positive for ALP. I, J, and K: In vivo diffusion chamber analysis of KUSA/A1 cells. Bone formation was detected not only inside the chamber but also outside the chamber, 4 weeks after transplantation. Note that calcium deposition was also observed outside the membrane as well as inside the membrane. I and J: H&E stain. K: von Kossa stain. Scale bars: 160 (A and B), 340 (C), 160 (D), 340 (E), 400 (F), 290 (G), 150 (G, inlet), 60 (H), 90 (I), 140 μm (J and K).
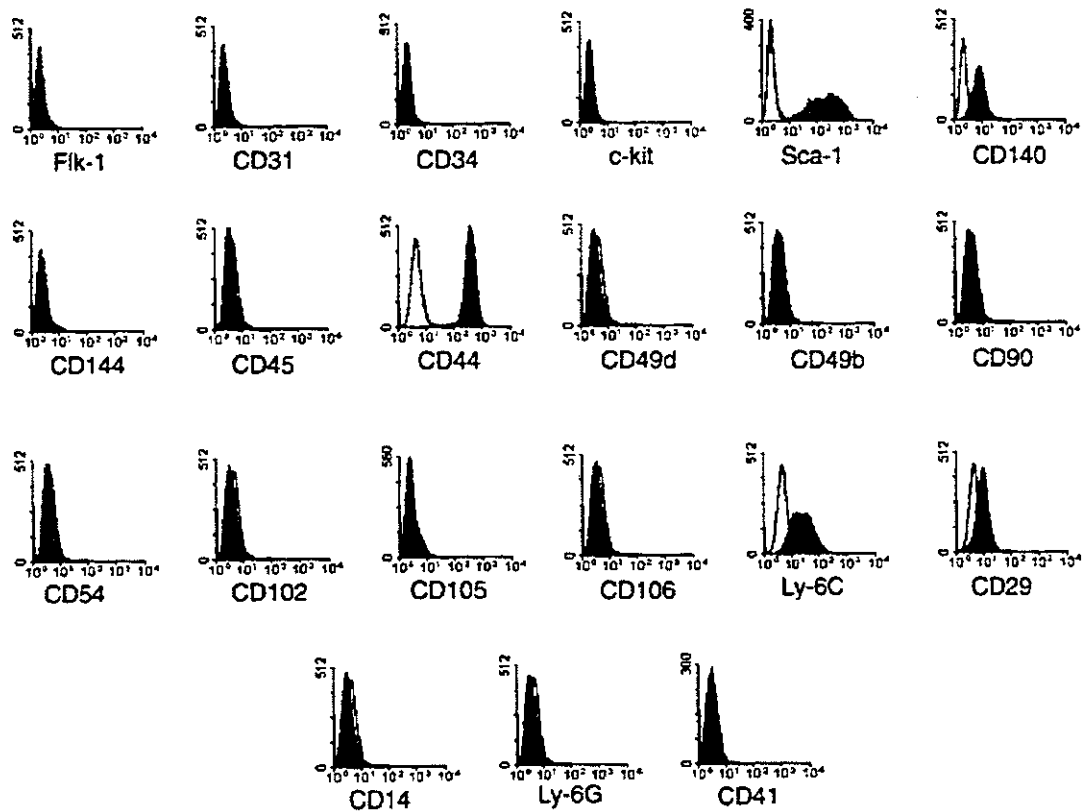
OCHI ET AL.

Fig. 4. Flow cytometry analysis of cell surface markers in KUSA/A1 cells. Cells stained with primary antibodies to Flk-1, CD31, CD34, c-kit, Sca-1, CD140, CD144, CD45, CD44, CD49d, CD49b, CD90, CD54, CD102, CD105, CD106, Ly-6C, CD29, CD14, Ly-6G, and CD41, are shown as gray peaks. The isotope controls are shown as white peaks.

cells were cultured for more than 5 days postconfluence. The inoculated cells were negative for calcium deposition on day 1 after the inoculation. But, bone matrix positive for von Kossa stain appeared in the injected cells on day 2, and had markedly increased and become larger, and the matrix became strongly positive for von Kossa stain on day 3. Marrow cavities were formed inside the bone generated by KUSA/A1 cells at 8 weeks and at later stages after inoculation. Hematopoietic cells were also observed in these bone marrow, as reported previously (Umezawa et al., 1992). No cartilage was formed in any KUSA/A1-transplanted bones, indicating that osteogenesis by KUSA/A1 is membranous ossification rather than enchondral ossification.

We continued to observe the fate of KUSA/A1 bone transplanted into the subcutaneous tissue and abdominal cavity, and found that the ectopic KUSA/A1 bone remained unchanged in size and shape for 12 months at both sites. Histologically, complete functional hematopoiesis by ectopic KUSA/A1 bone was seen in the subcutaneous tissue but not in the abdominal cavity.

Osteogenesis was directly generated by the inoculated KUSA/A1 osteoblasts

To determine whether these bones were directly formed by KUSA/A1 cells or generated by host-derived cells, we labeled KUSA/A1 cells with bacteria-derived

β-galactosidase (Fig. 3F−H). Frozen tissue sections showed that osteoblasts in the bone were positive for β-galactosidase. The osteoblastic cells, which exhibited strong β-galactosidase activities were also strongly positive for ALP. Sarcomatous proliferation of the inoculated cells, which were positive for β-galactosidase was not seen around the generated bone.

We also injected KUSA/A1 cells into a diffusion chamber and examined osteogenesis (Fig. 3I−K). This was performed to determine whether these bones were directly formed by KUSA/A1 cells or generated by host-derived cells, and whether osteogenesis requires direct cell−cell interactions with the adjacent cells. Diffusion chambers containing KUSA/A1 cells were transplanted subcutaneously into mice. Bone was formed inside the chamber 2 weeks after the transplantation and had calcium deposition. This bone formation became more evident from 4 weeks after the inoculation. Surprisingly, we observed bone formation even outside the chamber in specimens taken at 4 weeks. Calcification was also seen both inside and outside the chamber, suggesting that remarkably strong osteogenic soluble factors or cytokines were being secreted from KUSA/A1 cells. Interestingly, calcium deposition was also reproducibly detected in the membrane. Therefore, osteogenesis is induced directly by KUSA/A1 cells rather than indirectly by neighboring cells.
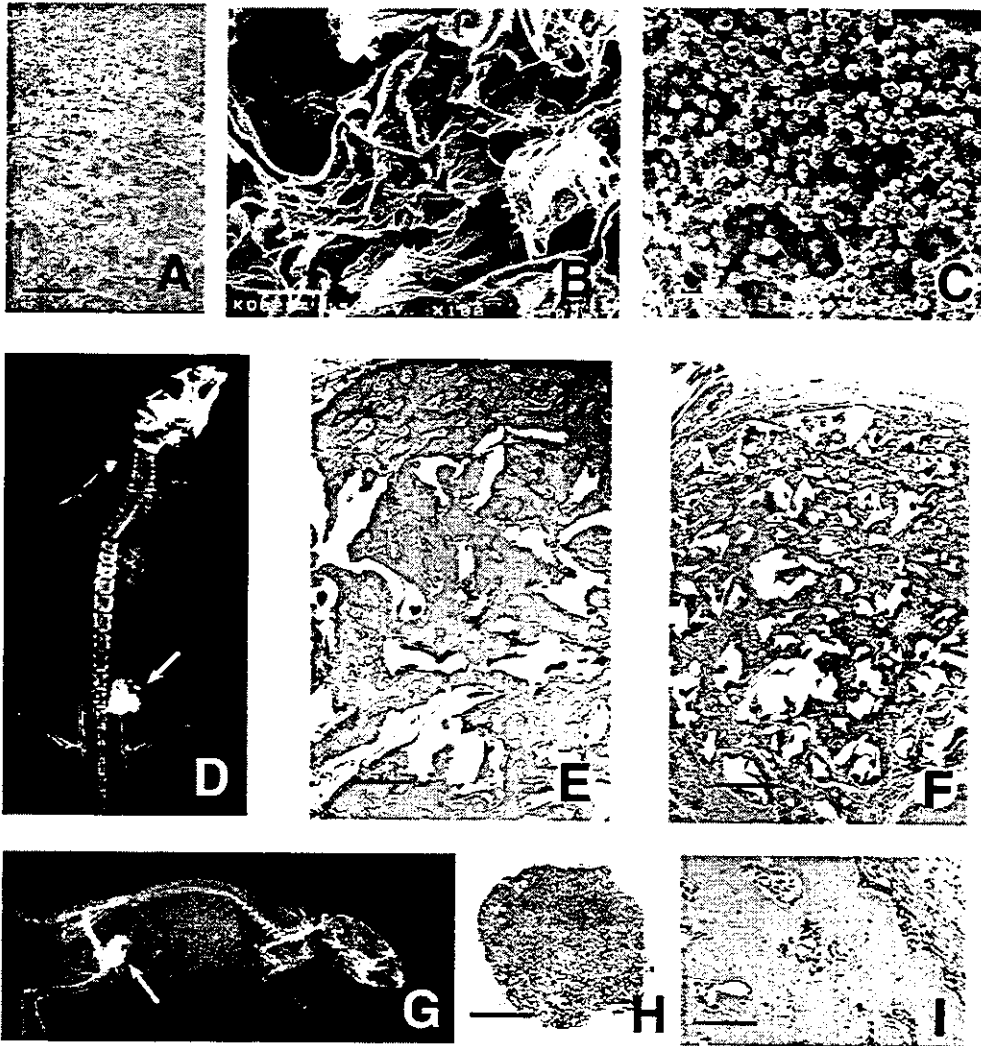
Fig. 5. Generation of custom-shaped bone by KUSA/A1 cells with PLGA-collagen sponge. PLGA-collagen sponge was used as a scaffold for KUSA/A1 cells. A: Macroscopic view of PLGA-collagen sponge. B: SEM of surface morphology of PLGA-collagen sponge without cells. C: SEM of PLGA-collagen sponge, into which KUSA/A1 cells were implanted. PLGA-collagen sponge, into which KUSA/A1 cells were implanted, was transplanted into the syngeneic mice. Six (D–F) or 11 (G–I) weeks after the transplantation, the KUSA/A1 in the sponge was excised for analysis. D: Soft X-ray of KUSA/A1 bone that is seen as an electron-dense, cuboidal bone. E: Histological examination of the bone generated by KUSA/A1 and PLGA-collagen sponge. Bone trabeculae were clearly seen. F: Histological examination of transplanted PLGA-collagen sponge without cells. Note that foreign body reaction was seen inside the transplanted sponge, but no bone was formed. G: Photo for soft X-ray of complete cuboidal bone by KUSA/A1 and PLGA-collagen sponge. H: Histology of complete cuboidal bone with high density of bone trabeculae. Note that bone was formed even in the center of the sponge. I: High power view of H. Scale bars: 350 (A), 100 (B), 72 (C), 200 μm (E and F), 5 mm (H), 250 μm (I).

Surface marker expression on KUSA/A1 cells

We analyzed the cell surface markers on the clonal KUSA/A1 cells by flow cytometry to better characterize these cells. Cells were incubated with monoclonal antibodies. Controls included cells stained with individual isotype (mouse IgG1 or rat IgG2a). Incubations were performed in the presence of mouse immunoglobulin to prevent nonspecific antibody binding. The cells were found to be strongly positive (more than tenfold greater than the isotype control) for Sca-1, CD44, Ly-6C and CD140, weakly positive for CD29, and negative for c-kit, Flk-1, CD14, CD31, CD34, CD41, CD45, CD49b, CD49d, CD54, CD90, CD102, CD105, CD106, CD144 and Ly-6G (Fig. 4). Surface marker analysis of KUSA/A1 indicated that cells with strong in vivo osteogenic activity exhibited markers for osteocytes (Horowitz et al., 1994; Hughes et al., 1994; Chen et al., 1999); CD44 and Ly-6C. Interestingly, the lack of CD90 expression supported the assumption that these cells maintain a matured phenotype even when they proliferate, since CD90 is detected in the early stage of osteoblast differentiation and declines as osteoblasts mature into osteocytes. Therefore, KUSA/A1 cells, which have strong in vivo osteogenic activity, express markers for mature osteoblasts or osteocytes. This was

confirmed with the cytochemical analysis of KUSA/A1 cells in vivo and in vitro. High ALP activity, calcium deposition, and osteocalcin release with low PTH responsibility also indicate that KUSA/A1 cells are mature osteoblasts or osteocytes.

Generating custom-shaped bones derived from KUSA/A1 cells in vivo with PLGA-collagen sponge

We attempted to generate bone tissue of desired sizes and shapes with a view to future clinical applications (Fig. 5). We previously developed a PLGA-collagen sponge with a pore of specific size for this purpose (Chen et al., 2000a,b). Collagen gels suspended with KUSA/A1 cells were injected into a cube of PLGA-collagen sponge, which was then transplanted into subcutaneous tissue and the abdominal cavity. Two weeks after the transplantation, cuboidal bone was seen on X-ray and formation of bone trabeculae was confirmed histologically. This bone formation was evident at 6 weeks. At 11 weeks, the PLGA sponge turned completely to bone. Hematopoietic cells and tartaric acid-resistant acid phosphatase-positive osteoclasts were also observed in the generated bone. Control PLGA sponges without any cells transplanted into both subcutaneous tissue and abdominal cavity showed no evidence of calcification or ossification.

DISCUSSION
Establishment of rapid and efficient membranous osteogenesis system by mature osteoblasts

We have devised and tested a system for regeneration of bone of specific shape and size that can be successfully implanted into mice using a clonal mature osteoblast cell line. These cells consistently differentiate to form bone both in vitro and in vivo. Very rapid, within 2 days, in vivo bone formation was obtained using mature KUSA/A1 osteoblasts that were cultured for 5–7 days at confluence before implantation. Cells implanted at semiconfluence, in contrast, took 2 weeks to generate bone (Umezawa et al., 1992). Since osteoprogenitor cells divide early in culture and have a limited capacity for self-renewal (McCulloch et al., 1991), these results suggest that use of mature osteoblasts is prerequisite for rapid bone formation in vivo. The in vivo osteogenic activity of the KUSA/A1 cells seems to be at least mediated by humoral factors produced by the cells per se, since bone formed not only inside the diffusion chamber but also outside the chamber, when the cells were transplanted into the chamber.

It would be interesting to assess the possibility of using mature osteoblasts as a therapeutic agent. Injection of isolated mature osteoblasts into a bone defect or fracture site would be more efficient means of accelerating bone fusion with minimal invasion than injection of all types of marrow cells into fracture sites.

PLGA-collagen sponge gave control over the shape and size of osteogenesis

We hypothesized that provision of a scaffold may effectively limit and guide new bone formation. Inoculation of KUSA/A1 cells cultured in collagen gel successfully induced bone in vivo, but collagen gel is too soft to maintain any specific desired shape in vivo, especially at

the site of bone defects. However, the PLGA-collagen sponge could both support osteoblast-mediated bone formation and retain its shape in vivo. PLGA-collagen sponge has a number of advantages as a scaffold for bone regeneration: (a) it is easily shaped; (b) the time course of degradation, mechanical strength, and plasticity can be easily modulated by changing the ratio of PLA and PGA; (c) it has a high affinity for cells, mediated by collagen; (d) cells can be injected evenly throughout the sponge so that the sponge turns completely to bone.

In regenerating articular cartilage, it is an important issue how to make mechanically strong, fully weight-bearing cartilage. To this end, subchondral bone, which undercoats cartilage and confers mechanical strength to articular cartilage needs to be generated. Cartilage has been successfully regenerated, however, connection between bone and regenerated cartilage was incomplete. Our present studies suggest that osteoblasts in a scaffold serve a possible candidate for a glue to bind subchondral bone and regenerated cartilage.

Importantly, custom-shaped bone regeneration using mature osteoblasts proved to be successful. Furthermore, transplanted KUSA/A1 cells did not transform into malignant cells, form any abnormal extracellular matrices, or induce any significant inflammatory reactions. The next step will be to isolate human counterparts to these mouse cell lines. Cell separation of osteoblasts from human marrow stroma and inoculation of the cells with appropriate scaffold will provide us a new ways of osteogenesis engineering.

LITERATURE CITED

Amagai M, Inokuchi Y, Nishikawa T, Shimizu Y, Shimizu N. 1989. Cloning of TPA-inducible early (TIE) genes by differential hybridization using TPA-nonresponsive variant of mouse 3T3-L1 cells. Somat Cell Mol Genet 15:153–158.

Bianco P, Robey PG. 2000. Marrow stromal stem cells. J Clin Invest 105:1663–1668.

Canalis E. 2000. Novel treatments for osteoporosis. J Clin Invest 106:177–179.

Chen XD, Qian HY, Neff L, Satomura K, Horowitz MC. 1999. Thy-1 antigen expression by cells in the osteoblast lineage. J Bone Miner Res 14:362–375.

Chen G, Ushida T, Tateishi T. 2000a. A biodegradable hybrid sponge nested with collagen microsponges. J Biomed Mater Res 51:273–279.

Chen G, Ushida T, Tateishi T. 2000b. Hybrid biomaterials for tissue engineering: A preparative method for PLA or PLGA-collagen hybrid sponges. Adv Mater 12:455–457.

Dexter TM, Allen TD, Lajtha LG. 1977. Conditions controlling the proliferation of haemopoietic stem cells in vitro. J Cell Physiol 91:335–344.

Feinberg AP, Vogelstein B. 1983. A technique for radiolabeling DNA restriction endonuclease fragments to high specific activity. Anal Biochem 132:6–13.

Horowitz MC, Fields A, DeMeo D, Qian HY, Bothwell AL, Trepman E. 1994. Expression and regulation of Ly-6 differentiation antigens by murine osteoblasts. Endocrinology 135:1032–1043.

Horwitz EM, Prockop DJ, Fitzpatrick LA, Koo WW, Gordon PL, Neel M, Sussman M, Orchard P, Marx JC, Pyeritz RE, Brenner MK. 1999. Transplantability and therapeutic effects of bone marrow-derived mesenchymal cells in children with osteogenesis imperfecta. Nat Med 5:309–313.

Hughes DE, Salter DM, Simpson R. 1994. CD44 expression in human bone: A novel marker of osteocytic differentiation. J Bone Miner Res 9:39–44.

Kohyama J, Abe H, Shimazaki T, Koizumi A, Nakashima K, Gojo S, Taga T, Okano H, Hata J, Umezawa A. 2001. Brain from bone: Efficient 'meta-differentiation' of marrow stroma-derived mature osteoblasts to neurons with Noggin or a demethylating agent. Differentiation 68:235–244.

Krebsbach PH, Kuznetsov SA, Satomura K, Emmons RV, Rowe DW, Robey PG. 1997. Bone formation in vivo: Comparison of osteogenesis by transplanted mouse and human marrow stromal fibroblasts. Transplantation 63:1059–1069.

Krebsbach PH, Mankani MH, Satomura K, Kuznetsov SA, Robey PG. 1998. Repair of craniotomy defects using bone marrow stromal cells. Transplantation 66:1272–1278.

Leboy PS, Beresford JN, Devlin C, Owen ME. 1991. Dexamethasone induction of osteoblast mRNAs in rat marrow stromal cell cultures. J Cell Physiol 146:370–378.

Makino S, Fukuda K, Miyoshi S, Konishi F, Kodama H, Pan J, Sano M, Takahashi T, Hori S, Abe H, Hata J, Umezawa A, Ogawa S. 1999. Cardiomyocytes can be generated from marrow stromal cells in vitro. J Clin Invest 103:697–705.

McCulloch CA, Strugurescu M, Hughes F, Melcher AH, Aubin JE. 1991. Osteogenic progenitor cells in rat bone marrow stromal populations exhibit self-renewal in culture. Blood 77:1906–1911.

Ohgushi H, Caplan AI. 1999. Stem cell technology and bioceramics: From cell to gene engineering. J Biomed Mater Res 48:913–927.

Pittenger MF, Mackay AM, Beck SC, Jaiswal RK, Douglas R, Mosca JD, Moorman MA, Simonetti DW, Craig S, Marshak DR. 1999. Multilineage potential of adult human mesenchymal stem cells. Science 284:143–147.

Pittenger MF, Mosca JD, McIntosh KR. 2000. Human mesenchymal stem cells: Progenitor cells for cartilage, bone, fat and stroma. Curr Top Microbiol Immunol 251:3–11.

Rodan GA, Martin TJ. 2000. Therapeutic approaches to bone diseases. Science 289:1508–1514.

Sato K, Han DC, Ozawa M, Fujii Y, Tsushima T, Shizume K. 1987. A highly sensitive bioassay for PTH using ROS 17/2.8 subclonal cells. Acta Endocrinol (Copenh) 116:113–120.

Service RF. 2000. Tissue engineers build new bone. Science 289:1498–1500.

Tabata Y, Hong L, Miyamoto S, Miyao M, Hashimoto N, Ikada Y. 2000. Bone formation at a rabbit skull defect by autologus bone marrow combined with gelatin microspheres containing TGF-beta1. J Biomater Sci Polym Ed 11:891–901.

Umezawa A, Tachibana K, Harigaya K, Kusakari S, Kato S, Watanabe Y, Takano T. 1991. Colony-stimulating factor 1 is downregulatd during the adipocyte differentiation of H-1/A marrow stromal cells and induced by cachectin/tumor necrosis factor. Mol Cell Biol 11:920–927.

Umezawa A, Maruyama T, Segawa K, Shadduck RK, Waheed A, Hata J. 1992. Multipotent marrow stromal cell line is able to induce hematopoiesis in vivo. J Cell Physiol 151:197–205.

Urist MR, Mizutani H, Conover MA, Lietze A, Finerman GA. 1982. Dentin, bone, and osteosarcoma tissue bone morphogenetic proteins. Prog Clin Biol Res 101:61–81.

Yamaguchi A, Komori T, Suda T. 2000. Regulation of osteoblast differentiation mediated by bone morphogenetic proteins, hedgehogs, and Cbfa1. Endocr Rev 21:393–411.

Yamashita T, Tonoki H, Nakata D, Yamano S, Segawa K, Moriuchi T. 1999. Adenovirus type 5 E1A immortalizes primary rat cells expressing wild-type p53. Microbiol Immunol 43:1037–1044.